Title for citation

SCIENCE CHINA
Information Sciences

• Supplementary File •

Additive-state-decomposition-based station-keeping control for autonomous aerial refueling

Jinrui Ren, Quan Quan*, Haibiao Ma & Kai-Yuan Cai

School of Automation Science and Electrical Engineering, Beihang University, Beijing 100191*, China*

Appendix A Proof of Theorem 4

For the longitudinal channel, according to *Theorem 3*, observer (14) will make $\hat{\tilde{\mathbf{x}}}_{\mathrm{rlon,p}} \equiv \tilde{\mathbf{x}}_{\mathrm{rlon,p}}$, $\hat{\tilde{\mathbf{x}}}_{\mathrm{rlon,s}} \equiv \tilde{\mathbf{x}}_{\mathrm{rlon,s}}$ and $\hat{\tilde{\mathbf{y}}}_{\mathrm{rlon,p}} \equiv \tilde{\mathbf{y}}_{\mathrm{rlon,p}}$. Under condition (i), the controller $\tilde{\mathbf{u}}_{\mathrm{rlon,p}}$ drives $\tilde{\mathbf{y}}_{\mathrm{rlon,p}}(t) - \tilde{\mathbf{y}}^{\mathrm{d}}_{\mathrm{rlon}}(t) \to \mathbf{0}$ as $t \to \infty$ for system (5) (*Theorem 1*), and the controller $\tilde{\mathbf{u}}_{\mathrm{rlon,s}}$ drives $\tilde{\mathbf{x}}_{\mathrm{rlon,s}} \to \mathbf{0}$ as $t \to \infty$ for system (6) (*Theorem 2*). Then the controller $\tilde{\mathbf{u}}_{\mathrm{rlon}} = \tilde{\mathbf{u}}_{\mathrm{rlon,p}} + \tilde{\mathbf{u}}_{\mathrm{rlon,s}}$ guarantees $\tilde{\mathbf{y}}_{\mathrm{rlon}}(t) - \tilde{\mathbf{y}}^{\mathrm{d}}_{\mathrm{rlon}}(t) \to \mathbf{0}$ as $t \to \infty$. For the lateral channel, it can be concluded that the controller $\tilde{\mathbf{u}}_{\mathrm{rlat}} = \tilde{\mathbf{u}}_{\mathrm{rlat,p}} + \tilde{\mathbf{u}}_{\mathrm{rlat,s}}$ guarantees $\tilde{\mathbf{y}}_{\mathrm{rlat}}(t) - \tilde{\mathbf{y}}^{\mathrm{d}}_{\mathrm{rlat}}(t) \to \mathbf{0}$ as $t \to \infty$ in a similar way. Then the controller $\tilde{\mathbf{u}}_{\mathrm{r}} = \tilde{\mathbf{u}}_{\mathrm{r,p}} + \tilde{\mathbf{u}}_{\mathrm{r,s}}$ guarantees $\tilde{\mathbf{y}}_{\mathrm{r}}(t) - \tilde{\mathbf{y}}^{\mathrm{d}}_{\mathrm{r}}(t) \to \mathbf{0}$ as $t \to \infty$ for system (2). □

Appendix B Simulation

In this part, the feasibility and the performance of the proposed ASD-based station-keeping controller are investigated through the simulation.

Simulation configuration

A MATLAB/SIMULINK-based simulation environment with a three-dimensional virtual-reality display has been developed by the authors' research laboratory to simulate the PDR. The detailed information about the modeling procedure, model parameters, and simulation environment can refer to previous works [1], [2].

In the simulation, the trim condition is the level and forward flight with the height $h_{\mathrm{r}} = 3000$m (9843ft) and the velocity $v_{\mathrm{r}} = 120$m/s (393.72ft/s). All the trimmed states are $\mathbf{x}_{\mathrm{r}} = \begin{bmatrix} 0 & 0 & 9843 & 0 & 0.1156 & 0 & 391 & 0 & 45 & 0 & 0 & 0 \end{bmatrix}^{\mathrm{T}}$ and all the trimmed inputs are $\mathbf{u}_{\mathrm{r}} = \begin{bmatrix} 2279.0852 & -2.9797 & 0.0087 & 0.0680 \end{bmatrix}^{\mathrm{T}}$. Controller parameters are set as follows.

Longitudinal-channel primary controller parameters:

$$\mathbf{Q}_{\mathrm{rlon}} = \mathrm{diag}\left(4, 10, 10, 1, 10, 10, 1, 3\right), \mathbf{R}_{\mathrm{rlon}} = \mathrm{diag}\left(50, 50\right)$$

$$\mathbf{K}_{\mathbf{x}\mathrm{lon}} = \begin{bmatrix} 0.6690 & 0.1816 & 72.926 & 1.3386 & -75.589 & 1.0669 \\ 0.0974 & -0.7903 & -354.56 & 0.0628 & 246.25 & -50.082 \end{bmatrix}, \mathbf{K}_{\mathbf{e}\mathrm{lon}} = \begin{bmatrix} 0.1392 & 0.0433 \\ 0.0250 & -0.2411 \end{bmatrix}$$

Longitudinal-channel secondary controller parameters:

$$\mathbf{C}_{\mathrm{slon}} = \begin{bmatrix} -14.068 & 196.526 & 143428.581 & 2406.307 & -147654.857 & 2428.098 \\ 194.075 & 76.508 & 44066.609 & 904.369 & -48027.709 & -41.490 \end{bmatrix}, \mathbf{K}_{\mathrm{rlon}} = \begin{bmatrix} 1 & 0 \\ 0 & 1 \end{bmatrix}$$

Lateral-channel primary controller parameters:

$$\mathbf{Q}_{\mathrm{rlat}} = \mathrm{diag}\left(10, 2, 4, 4, 2, 2, 4\right), \mathbf{R}_{\mathrm{rlat}} = \mathrm{diag}\left(50, 50\right)$$

$$\mathbf{K}_{\mathbf{x}\mathrm{lat}} = \begin{bmatrix} -0.3833 & 9.6773 & -287.58 & -250.74 & -5.7648 & -34.536 \\ -0.0867 & 2.1597 & -70.513 & -61.301 & -1.4822 & -8.9008 \end{bmatrix}, \mathbf{K}_{\mathbf{e}\mathrm{lat}} = \begin{bmatrix} -0.0876 \\ -0.0180 \end{bmatrix}$$

Lateral-channel secondary controller parameters:

$$\mathbf{C}_{\mathrm{slat}} = \begin{bmatrix} -1.272 & 55.046 & -880.467 & -775.037 & -7.652 & -52.170 \\ -0.143 & 9.216 & -173.189 & -149.751 & -1.826 & -13.936 \end{bmatrix}, \mathbf{K}_{\mathrm{rlat}} = \begin{bmatrix} 1 & 0 \\ 0 & 1 \end{bmatrix}$$

* Corresponding author (email: qq_buaa@buaa.edu.cn)

Simulation 1: Station-keeping with constant mass

In the first group of simulations, the joining phase from the standby point A to the observation position B and the pre-refueling phase from B to the pre-contact point C are studied. During these phases, the receiver mass remains unchanged. The position A is set as $\mathbf{p}_{\mathrm{r0}}^{\mathrm{t}} = \begin{bmatrix} -60 & -50 & 5 \end{bmatrix}^{\mathrm{T}}$, the position B is set as $\mathbf{p}_{\mathrm{r1}}^{\mathrm{t}} = \begin{bmatrix} -10 & -50 & 5 \end{bmatrix}^{\mathrm{T}}$, and the position C is set as $\mathbf{p}_{\mathrm{r2}}^{\mathrm{t}} = \begin{bmatrix} -25 & 0 & 5 \end{bmatrix}^{\mathrm{T}}$ in the tanker frame. The total simulation time is $T = 200$s. The first phase from A to B begins when $t = 10$s, and the second phase from B to C begins when $t = 90$s. First, when the tanker vortex is considered, the tracking response is presented in Fig. B1. During the beginning 10s, the receiver stays relatively still to the tanker. Then, the receiver moves forward slowly, and reaches the observation position B at about 75s. After staying still for 15s, the receiver begins to move backward and to the right to approach C, and gets there at about 160s. It can also be seen that, during the whole flight, the receiver tracks the reference trajectory well. The actual flight trajectory is smooth, and the steady-state error is zero. The corresponding control inputs including the thrust and the actuator deflection are displayed in Fig. B2. Other nine states are displayed in Fig. B3. They all meet the control requirements. Then, taking the atmospheric turbulence into consideration, the tracking response is presented in Fig. B4. The maximum velocity of the induced wind field by the atmospheric turbulence can reach 1m/s. Under this circumstance, the receiver tracks the reference trajectory under slight fluctuation. The whole tracking effect is satisfactory. Thus, the designed controller can achieve good control effect in the presence of the wind disturbances.

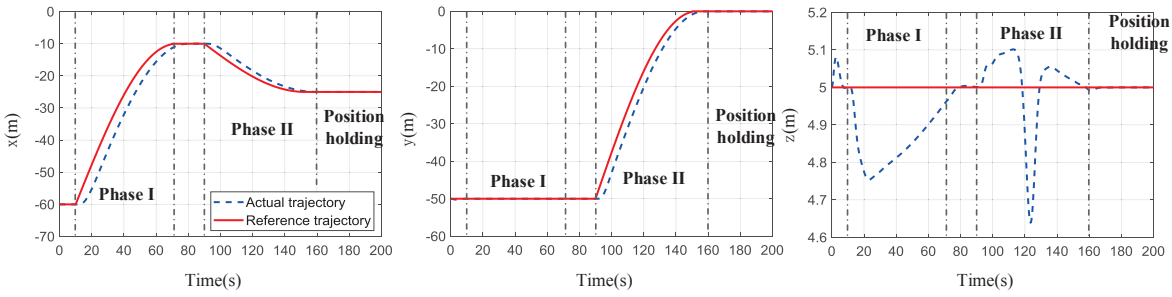

Figure B1 Trajectory tracking response under the tanker vortex.

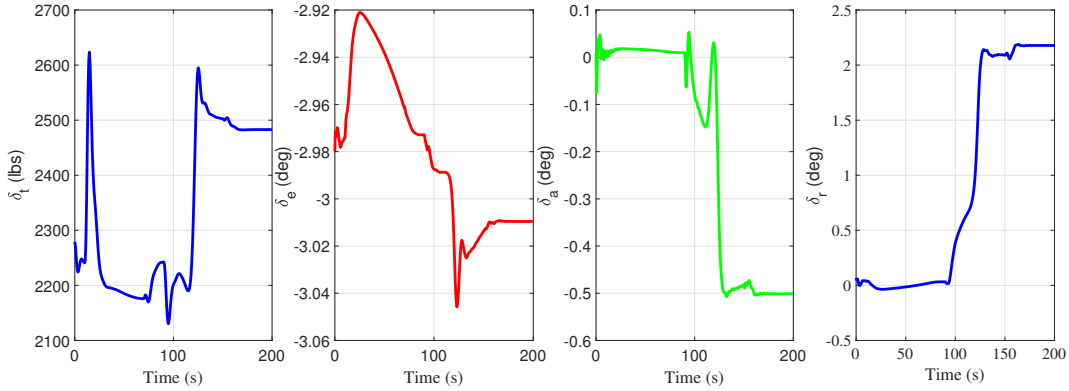

Figure B2 Control inputs.

Simulation 2: Station-keeping with varying mass

In the second group of simulations, the fuel transferring phase, namely the receiver and the tanker keep relatively stationary to transfer the fuel, is considered. During this phase, the receiver mass increases gradually as the fuel transfers. The receiver mass before fuel transfer is $m_0 = 9295$kg, and the receiver mass after fuel transfer is $m_1 = 11295$kg. Total 2000kg fuel is transferred. If the fuel transferring speed is $v_{\mathrm{ft}} = \dot{m} = 20$kg/s, then the fuelling time is $T_{\mathrm{ft}} = 100$s. Suppose that, in the tanker frame, the reference position of the receiver is $\mathbf{p}_{\mathrm{d}}^{\mathrm{t}} = \begin{bmatrix} -15 & 0 & 5 \end{bmatrix}^{\mathrm{T}}$. The position holding response is displayed in Fig. B5. It can be seen that the mass-varying receiver holds in the refueling position well and the response under varying mass is just slightly different from the response under the constant mass. This means the proposed controller has robustness against the receiver mass change.

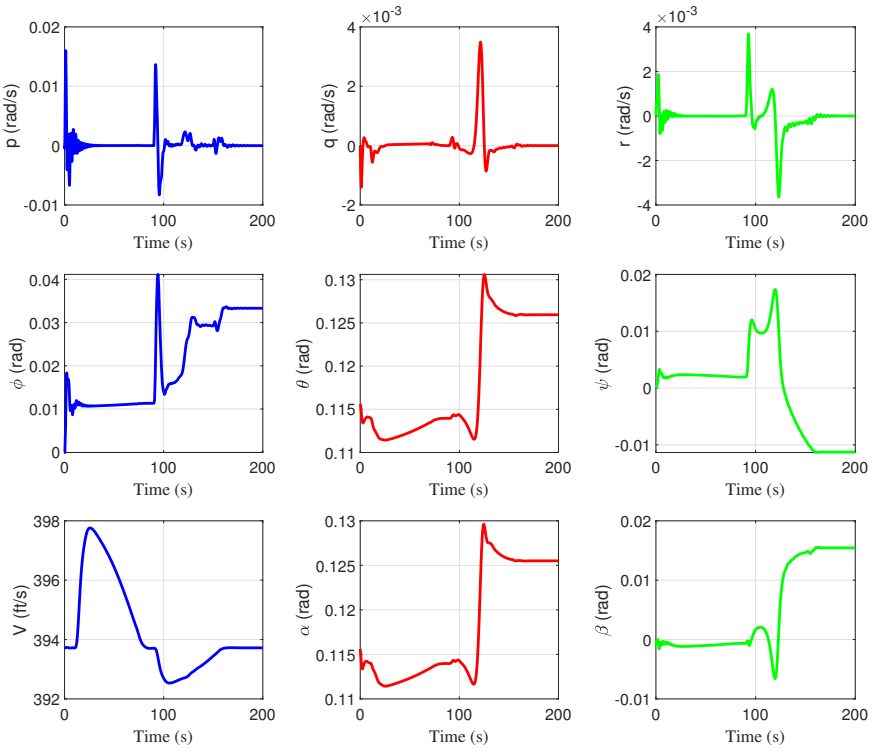

Figure B3 State response.

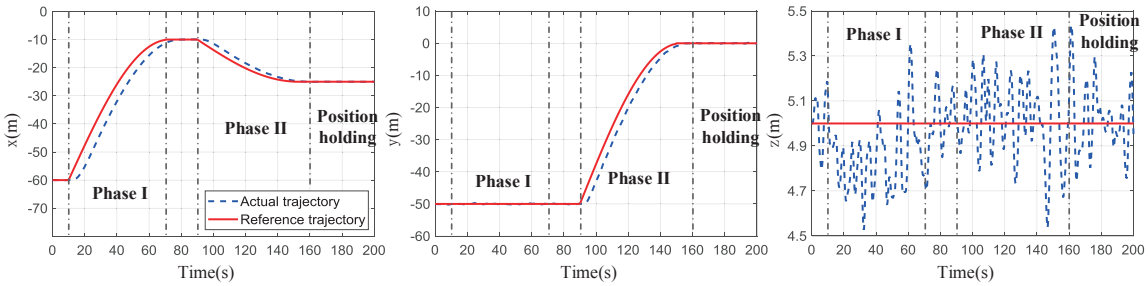

Figure B4 Trajectory tracking response under the atmospheric turbulence.

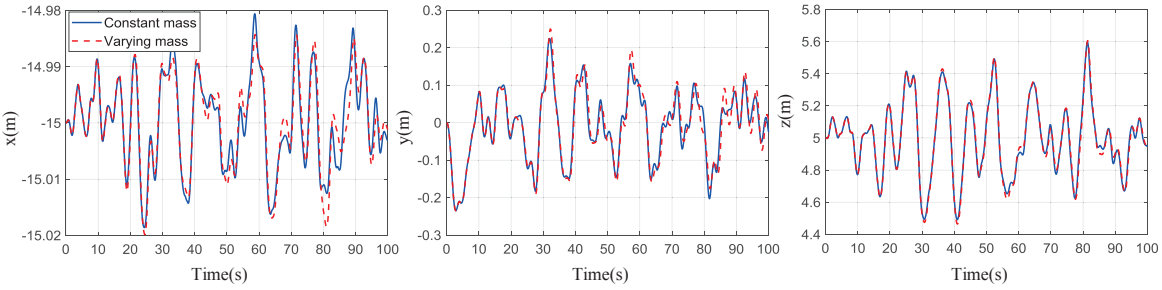

Figure B5 Position holding effect of the varying mass receiver.

References

1 Ren J, Dai X, Quan Q, et al. Reliable docking control scheme for probe drogue refueling. J Guidance Control Dyn, 2019, 42(11): 2511-2520

2 Wei Z B, Dai X, Quan Q, et al. Drogue dynamic model under bow wave in probe-and-drogue refueling. IEEE Trans Aerosp Electron Syst, 2016, 52(4): 1728-1742